PROCEEDINGS OF SCIENCE

Measurement of the atmospheric muon neutrino flux with KM3NeT/ORCA6

Dimitris Stavropoulos,[a,b,*] **Ekaterini Tzamariudaki,**[a] **Evangelia Drakopoulou**[a] **and Christos Markou**[a] **for the KM3NeT collaboration**

[a] *NCSR Demokritos, Institute of Nuclear and Particle Physics, Ag. Paraskevi Attikis, Athens, 15310 Greece*

[b] *National Technical University of Athens, School of Applied Mathematical and Physical Sciences, Zografou Campus, 9, Iroon Polytechniou str, 15780 Zografou, Athens, Greece*

E-mail: dstavropoulos@inp.demokritos.gr

The KM3NeT/ORCA detector (Oscillation Research with Cosmics in the Abyss) is an array of Digital Optical Modules, spheres that host 31 photomultiplier tubes, tied together in vertical structures, the Detection Units, which are anchored on the seabed. Such an array configuration can detect neutrino events from the Cherenkov radiation emitted by the secondary particles induced by neutrino interactions in the abyssal depths of the Mediterranean Sea. The KM3NeT/ORCA detector is being deployed at a depth of 2450 m offshore Toulon, France with the determination of the Neutrino Mass Ordering being the main physics goal of the detector. The aim of this work is the study of atmospheric neutrinos with energies at the 1-100 GeV range, in order to obtain information on the atmospheric muon neutrino flux in this energy range, in which only few measurements exist by other experiments. An analysis of data collected with the 6-Detection Unit configuration of KM3NeT/ORCA (KM3NeT/ORCA6) is being presented in this contribution. The data analyzed corresponds to a time period of one and a half year. The procedure for the selection of a high-purity atmospheric neutrino sample, using a Machine Learning classifier (Boosted Decision Tree), is described. Subsequently, an unfolding scheme is used to obtain an estimation of the atmospheric muon neutrino flux in bins of energy in the region of interest.

38th International Cosmic Ray Conference (ICRC2023)
26 July - 3 August, 2023
Nagoya, Japan

[*] Speaker

1. Introduction

Measurements of the atmospheric neutrino flux are increasingly important for testing the models that describe the production of the cosmic rays as well as their interaction mechanisms in the atmosphere. A reliable description of the atmospheric neutrino flux is also mandatory, as atmospheric neutrinos are used from several oscillation experiments. Moreover, a precise knowledge of the atmospheric neutrino flux is critical for constraining the contribution of this irriducible background source in the search of cosmic neutrinos. The prospects of KM3NeT/ORCA to contribute at the energy range between 1 GeV and 100 GeV has been already reported in [1]. In the following, a first measurement of the atmospheric muon neutrino flux is presented using data collected with KM3NeT/ORCA. This measurement illustrates the ability of the KM3NeT/ORCA detector, even with an early-stage detector configuration, to provide experimental information at an energy region in which only few measurements exist by other experiments.

2. The KM3NeT/ORCA detector

The KM3NeT Collaboration is currently constructing a research infrastructure in the depths of the Mediterranean Sea [2]. The ORCA detector (*Oscillation Research with Cosmics in the Abyss*), is under construction at a location ~ 40 km offshore Toulon, France, at a depth of 2450 m. ORCA is an array of photomultiplier tubes (PMTs) capable of detecting neutrino events via the Cherenkov radiation emmited by the daughter particles. When completed, it will consist of 115 Detection Units (DUs), vertical structures with 18 Digital Optical Modules (DOMs) each. The DOM is a sphere that hosts 31 3-inch PMTs as well as the required electronics [3] (Fig. 1). The distance between the DUs in ORCA is ~ 20 m, while the vertical distance between the DOMs in the same DU is ~ 9 m, so the height of the ORCA detector is ~ 160 m. At its final form, ORCA will have a cylinrical shape with ~ 100 m radius. ORCA is currently operating using 16 Detection Units.

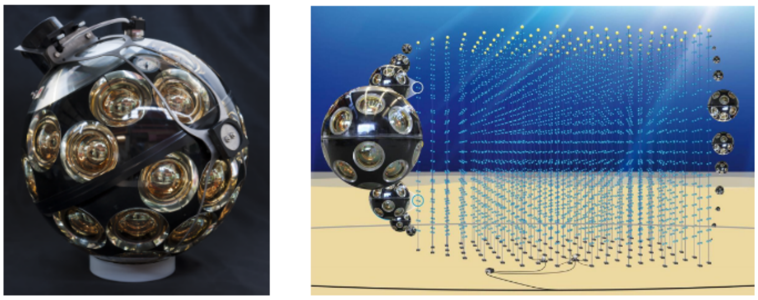

Figure 1: The Digital Optical Module (left) and an artistic view of the full KM3Net/ORCA detector (right).

3. Data and MC simulation

The data used in this analysis have been collected with the 6-DU configuration of the ORCA detector, referred to as ORCA6, which was operating from January-2020 to November-2021. The data livetime used for this analysis is equal to 555.7 days. This results in an ~ 84% time efficiency with respect to the total running time period for ORCA, as a fraction of the running time was devoted to calibration and test runs, and additional quality criteria were applied.

Monte Carlo (MC) event samples were produced to estimate the contribution of atmospheric muons and atmospheric neutrinos. The MUPAGE software has been used to generate atmospheric muon events [4]. Atmospheric neutrino events have been generated in the energy range between 1 GeV and 10 TeV using the gSeaGen software [5]. Charged current (CC) neutrino interactions have been simulated for all neutrino flavours, while the neutral current (NC) interactions of all flavours have been simulated and treated as a single component. The neutrino events have been weighted to account for the atmospheric neutrino flux and the oscillation probabilities. The HKKM14 atmospheric neutrino conventional flux model has been used [6]. For what concerns the neutrino oscillations, the parameters have been set according to NuFIT 5.2 [7], and oscillation probabilities have been computed assuming normal hierarchy. The light simulation as well as the PMT readout have been simulated using custom KM3NeT software.

The trigger algorithms that have been applied during the data acquisition as well as during the trigger level of the MC simulation, belong to the KM3NeT-specific Jpp software package [8]. The same software package has been used for the processing of triggered events in data and MC through the reconstruction chain (track and shower).

4. Event classification for a high-purity neutrino selection

The contribution of the random noise events, coming from optical backgrounds in sea water, is suppressed by applying a requirement on the likelihood and by requesting a minimum number of PMT hits contributing to the reconstructed track. Additionally, only events reconstructed with an upward-going direction are accepted.

The upward-going reconstructed events that survive these anti-noise cuts are further selected using a Boosted Decision Tree (BDT) algorithm. For this, the *TMVA* software is used [9]. Atmospheric $\nu_\mu + \bar{\nu}_\mu$ CC events are considered as signal, and atmospheric muons as background. 20 features are used for the BDT, and they are related to the reconstructed event position and direction, the reconstruction quality, and the event topology considering signal-like hits and charge distributions. The number of DOMs with at least one triggered hit, is also used. Dedicated MC event samples were produced to train and test the BDT algorithm.

The phase space of the BDT parameters has been scanned in order to find an optimal parameter set. For each set of parameters, the efficiency at indicative BDT score values as well as an overtraining check were performed, using an amount of $\sim 10\%$ of the data livetime. The optimal values of the chosen set of parameters, include the number of trees set to 400, the tree maximum depth to 6, and the adaptive boost parameter set to 0.3. The BDT score distributions for data and MC simulated events satisfying the anti-noise selection criteria and reconstructed as upgoing, are shown in Fig.2.

Good discrimination between the signal and background is achieved, as the former dominates at the higher score values, while the latter at the lower values. The requirement for an event to be included in the final selection is to have a BDT score greater or equal than 0.56. That leads to 4197 data events, while 4196.1 atmospheric $\nu + \bar{\nu}$ events are expected from MC simulation, from which 3214.8 are $\nu_\mu + \bar{\nu}_\mu$ CC events. The resulting contamination of atmospheric muon

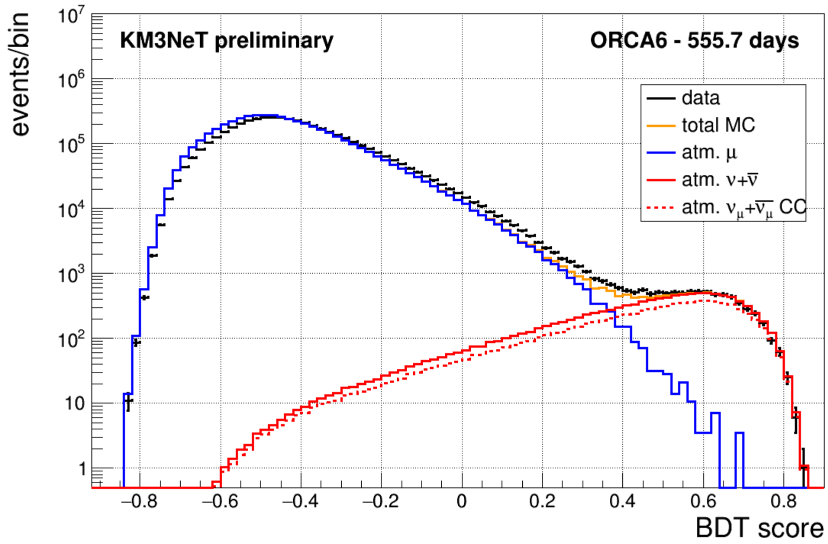

Figure 2: BDT score distributions for the upward-going ORCA6 events that survive the anti-noise criteria.

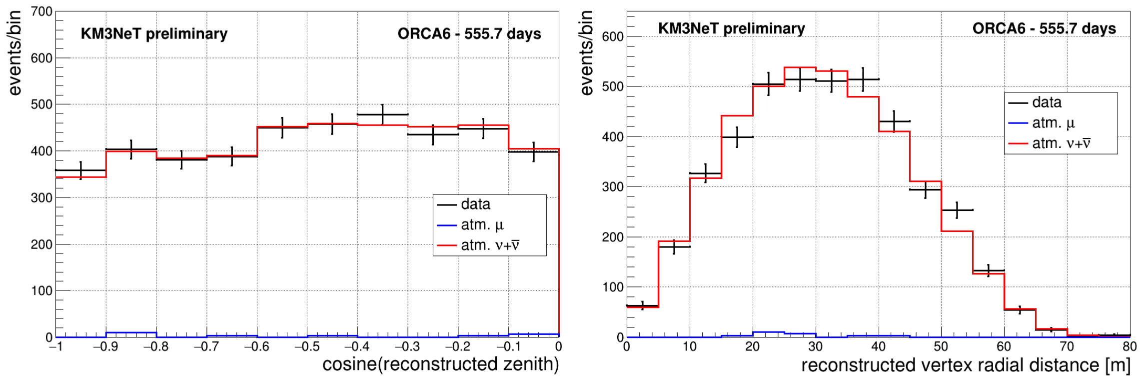

(a) Distribution of reconstructed cosine zenith. **(b)** Distribution of the reconstructed vertex radial distance.

Figure 3: Event variable distributions for the neutrino selection.

in the MC sample is estimated to be 28.1 events, which corresponds to 0.6% of the sample. A good agreement between data and MC simulation is obtained. The reconstructed cosine zenith distribution is presented in Fig.3a, for the BDT selected events. The distribution of the radial distance between the reconstructed vertex and the barycenter of the detector is also shown in Fig.3b.

5. Unfolding the $\nu_\mu + \bar{\nu}_\mu$ CC energy spectrum

An unfolding scheme is applied in order to deconvolute the $\nu_\mu + \bar{\nu}_\mu$ CC energy spectrum from the measured data energy distribution. For this, the *TUnfold* software is used [10]. In principle an unfolding scheme (with background subtraction) is described by:

$$y_i = \sum_{j=1}^{m} A_{ij} x_j + b_i, 1 \leq i \leq n \tag{1}$$

where y is the energy distribution for data, A the response matrix, x the true distribution which is being unfolded, and b the background contributions (can be more than one). The index i counts over the n bins of the reconstructed phase space while the index j counts over the m bins of the true phase space. *TUnfold* estimates the true x distribution using a least square method with Tikhonov regularization and an optional constraint [10]. Due to the limited size of the ORCA6 detector configuration, the shower reconstructed energy is used for unfolding the $\nu_\mu + \bar{\nu}_\mu$ CC energy spectrum.

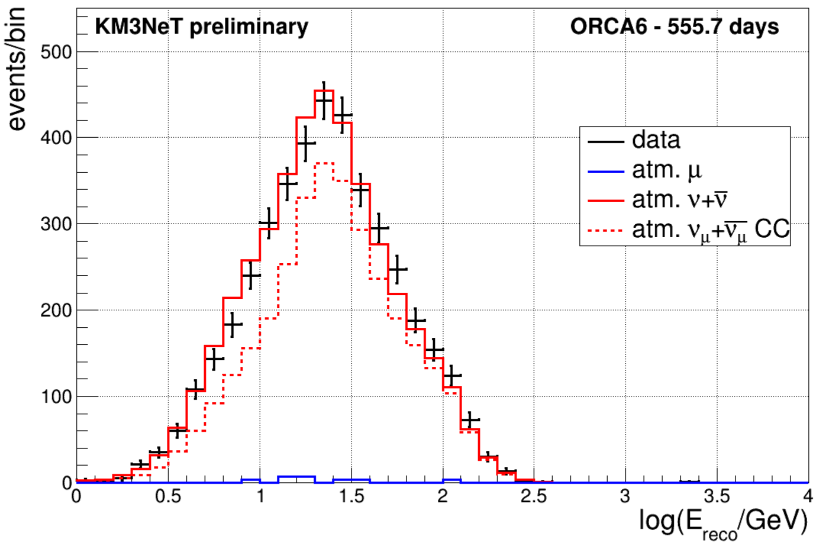

Figure 4: Reconstructed energy distribution for the selected events.

Only $\nu_\mu + \bar{\nu}_\mu$ CC are considered as signal events. Therefore, atmosperic muons, atmospheric $\nu_e + \bar{\nu}_e$ CC, atmospheric $\nu_\tau + \bar{\nu}_\tau$ CC and atmospheric $\nu + \bar{\nu}$ NC events are considered as background sources. In addition, atmospheric $\nu_\mu + \bar{\nu_\mu}$ CC with $E_{true} > 100$ GeV are also treated as background and their contribution is also subtracted from the reconstructed energy distribution. This approach was followed as the energy reconstruction is affected by the limited instrumented volume at this early-stage of construction. As a result, the flux measurement is performed in the range between 1 GeV-100 GeV. The consistency of the unfolding procedure was tested by replacing the reconstructed data distribution with the one for the atmospheric neutrino MC, and the robustness of the method was also checked by producing 1000 unfolding toy MC experiments. The bins used in this analysis were chosen taking the bin purity into account. The chosen binnings are $\{0.0, 0.1, 0.2, ..., 2.5, 2.6\}$ and $\{0.0, 0.8, 1.3, 1.8, 2.0\}$ for the reconstructed phase space and the true phase space respectively. The response matrix used for the unfolding procedure is shown in Fig.5.

After several tests which were performed exclusively using MC simulated events, to test the procedure and define the binning schemes, the unfolding was eventualy performed using the data

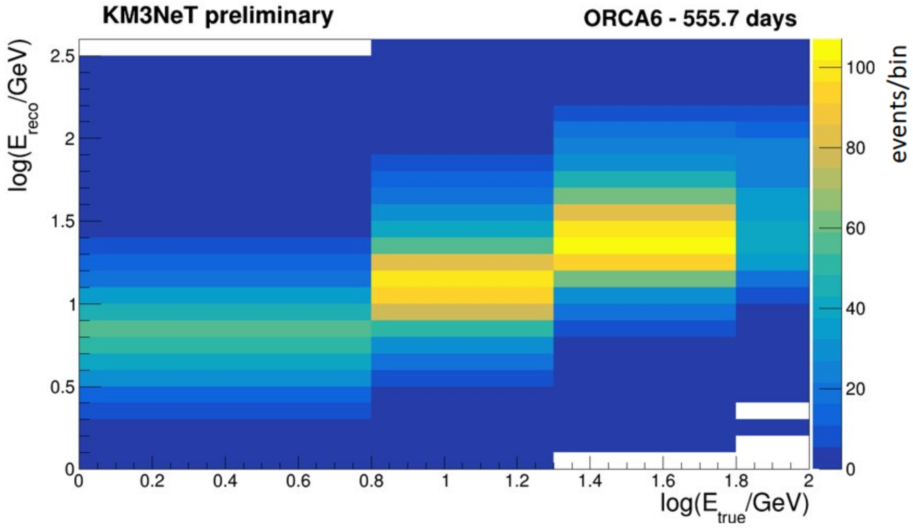

Figure 5: Response matrix for the event selection with the binning schemes used in the unfolding.

reconstructed energy distribution. The unfolded $\nu_\mu + \bar{\nu}_\mu$ CC energy distribution is presented in Fig.6, while the true $\nu_\mu + \bar{\nu}_\mu$ energy distribution has been also added as a reference.

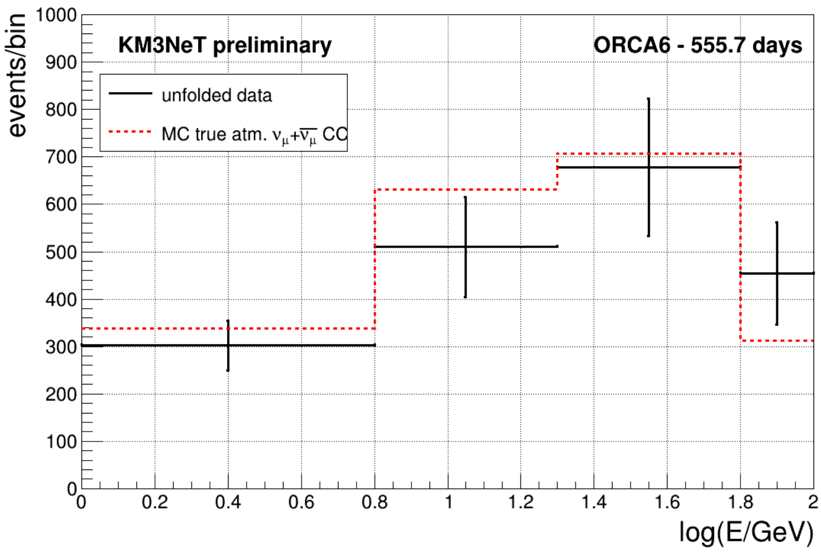

Figure 6: Unfolded energy distribution for the $\nu_\mu + \bar{\nu}_\mu$ CC events. The MC (true) $\nu_\mu + \bar{\nu}_\mu$ energy distribution is also shown as a reference.

6. Measurement of the flux

The last step is to convert the unfolded number of events per energy bin into flux values. The procedure is based on equation 2,

$$\Phi_i = \Phi_i^{MC} \cdot \frac{N_i^{unf}}{N_i^{MC}} \tag{2}$$

where Φ_i is the measured value for the bin i, Φ_i^{MC} is the flux value predicted by the HKKM14 atmospheric neutrino flux model [6], calculated at the weighted bin center for the bin i, N_i^{unf} is the number of events extracted by the unfolding scheme, and N_i^{MC} is the number of MC events in the bin. The value Φ_i^{MC} is calculated using the HKKM14 tabulated values are used, integrated over the azimuth angle, in order to integrate over the zenith angle according to equation 3, where $O^{\nu_i \to \nu_j}$ is the oscillation probability from ν_i to ν_j, set as in [7].

$$\begin{aligned}\Phi_{MC}^{\nu_\mu+\bar{\nu}_\mu}(E_\nu) = \int_{4\pi} d\Omega \Big\{ &\Phi_{MC}^{\nu_e}(E_\nu,\theta) \cdot O^{\nu_e \to \nu_\mu}(E_\nu,\theta) + \Phi_{MC}^{\bar{\nu}_e}(E_\nu,\theta) \cdot O^{\bar{\nu}_e \to \bar{\nu}_\mu}(E_\nu,\theta) \\ &+\Phi_{MC}^{\nu_\mu}(E_\nu,\theta) \cdot O^{\nu_\mu \to \nu_\mu}(E_\nu,\theta) + \Phi_{MC}^{\bar{\nu}_\mu}(E_\nu,\theta) \cdot O^{\bar{\nu}_\mu \to \bar{\nu}_\mu}(E_\nu,\theta) \Big\}\end{aligned} \tag{3}$$

The value of Φ_i^{MC} at the equation 2 is calculated by interpolating the integrated flux of equation 3 at the energy that corresponds to the weighted bin center for each bin. The results of the measurement are shown in Table 1. The errors are statistical only and are propagated from the results of the unfolding procedure.

$\Delta log(E_\nu/GeV)$	$\overline{log(E_\nu/GeV)}$	$E_\nu^2\Phi_\nu[GeV \cdot s^{-1} \cdot sr^{-1} \cdot cm^{-2}]$	stat.
0.0-0.8	0.39	$1.43 \cdot 10^{-2}$	±17%
0.8-1.3	0.93	$4.25 \cdot 10^{-3}$	±21%
1.3-1.8	1.45	$1.57 \cdot 10^{-3}$	±21%
1.8-2.0	1.88	$8.46 \cdot 10^{-4}$	±24%

Table 1: From left to right: Bin energy range; weighted energy bin center; flux measurement multiplied by the weighted energy bin center; statistical error.

The KM3NeT/ORCA6 measured flux values along with measurements from other experiments ([11],[12]) are presented in Fig.7. The measurement performed by Frejus on 1995 [13] is not shown in Fig.7 as it was done before the discovery of neutrino oscillations.

7. Conclusion

A measurement of the atmospheric muon neutrino flux using the first KM3NeT/ORCA data has been performed. The ability of ORCA to provide significant information concerning the atmospheric neutrino flux, even with an early-stage detector configuration, is shown in Fig.7. This measurement is in good agreement with the only existing and up-to-date one below 100 GeV, from Super-Kamiokande. A study for the estimation of the systematic uncertainties in this analysis is ongoing.

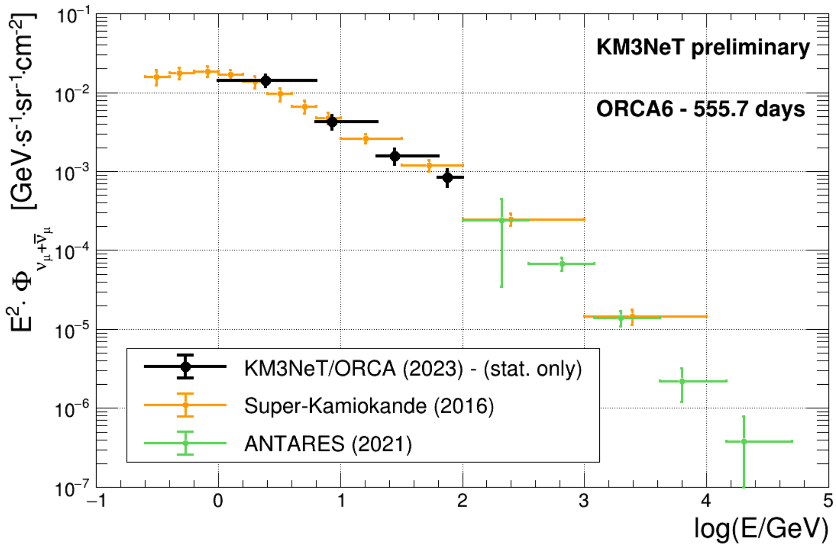

Figure 7: The atmospheric muon neutrino flux measurement using KM3NeT/ORCA6 data is shown along with other measurements.

References

[1] D. Stavropoulos, V. Pestel, Z. Aly, E. Tzamariudaki, C. Markou, PoS ICRC2021, 1125 (2021). https://doi.org/10.22323/1.395.1125

[2] S. Adrián-Martínez et al. (KM3NeT Collaboration), 2016 J. Phys. G43084001.

[3] S. Aiello et al. (KM3NeT Collaboration), The KM3NeT multi-PMT optical module, JINST 17 (2022) P07038.

[4] G. Carminati, A. Margiotta, M. Spurio, Comput. Phys. Commun.179, 915 (2008).

[5] S. Aiello et al. (KM3NeT Collaboration), Comput. Phys. Commun. 256, 107477 (2020)

[6] M. Honda et al., Phys. Rev. D 92, 023004 (2015), https://www.icrr.u-tokyo.ac.jp/mhonda/nflx2014/

[7] HEP 09 (2020) 178 [arXiv:2007.14792], NuFIT 5.2 (2022), www.nu-fit.org.

[8] K. Melis, A. Heijboer and M. de Jong (for the KM3NeT Collaboration), PoS(ICRC2017)950

[9] A. Hoecker, P. Speckmayer, J. Stelzer, J. Therhaag, E. von Toerne, and H. Voss, "TMVA: Toolkit for Multivariate Data Analysis," PoS A CAT 040 (2007) [physics/0703039].

[10] S.Schmitt, JINST 7 (2012) T10003 [arXiv:1205.6201]

[11] E. Richard, et al. Phys. Rev. D, 94 (2016) 052001

[12] Albert A., et al., ANTARES Collaboration Phys. Lett. B, 816 (2021) 136228,

[13] K. Daum (Frejus Collaboration), Z, Phys. C 66, 417 (1995)

Full Authors List: The KM3NeT Collaboration

S. Aiello[a], A. Albert[b,bd], S. Alves Garre[c], Z. Aly[d], A. Ambrosone[f,e], F. Ameli[g], M. Andre[h], E. Androutsou[i], M. Anguita[j], L. Aphecetche[k], M. Ardid[l], S. Ardid[l], H. Atmani[m], J. Aublin[n], L. Bailly-Salins[o], Z. Bardačová[q,p], B. Baret[n], A. Bariego-Quintana[c], S. Basegmez du Pree[r], Y. Becherini[n], M. Bendahman[m,n], F. Benfenati[t,s], M. Benhassi[u,e], D.M. Benoit[v], E. Berbee[r], V. Bertin[d], S. Biagi[w], M. Boettcher[x], D. Bonanno[w], J. Boumaaza[m], M. Bouta[y], M. Bouwhuis[r], C. Bozza[z,e], R.M. Bozza[f,e], H.Brânzaş[aa], F. Bretaudeau[k], R. Bruijn[ab,r], J. Brunner[d], R. Bruno[a], E. Buis[ac,r], R. Buompane[u,e], J. Busto[d], B. Caiffi[ad], D. Calvo[c], S. Campion[g,ae], A. Capone[g,ae], F. Carenini[t,s], V. Carretero[c], T. Cartraud[n], P. Castaldi[af,s], V. Cecchini[c], S. Celli[g,ae], L. Cerisy[d], M. Chabab[ag], M. Chadolias[ah], A. Chen[ai], S. Cherubini[aj,w], T. Chiarusi[s], M. Circella[ak], R. Cocimano[w], J.A.B. Coelho[n], A. Coleiro[n], R. Coniglione[w] P. Coyle[d], A. Creusot[n], A. Cruz[al], G. Cuttone[w], R. Dallier[k], Y. Darras[ah], A. De Benedittis[e], B. De Martino[d], V. Decoene[k], R. Del Burgo[e], U.M. Di Cerbo[e], L.S. Di Mauro[w], I. Di Palma[g,ae], A.F. Díaz[j], C. Diaz[j], D. Diego-Tortosa[w], C. Distefano[w], A. Domi[ah], C. Donzaud[n], D. Dornic[d], M. Dörr[am], E. Drakopoulou[i], D. Drouhin[b,bd], R. Dvornický[q], T. Eberl[ah], E. Eckerová[q,p], A. Eddymaoui[m], T. van Eeden[r], M. Eff[n], D. van Eijk[r], I. El Bojaddaini[y], S. El Hedri[n], A. Enzenhöfer[d], G. Ferrara[w], M. D. Filipović[an], F. Filippini[t,s], D. Franciotti[w], L.A. Fusco[z,e], J. Gabriel[ao], S. Gagliardini[g], T. Gal[ah], J. García Méndez[l], A. Garcia Soto[c], C. Gatius Oliver[r], N. Geißelbrecht[ah], H. Ghaddari[y], L. Gialanella[e,u], B.K. Gibson[v], E. Giorgio[w], I. Goos[n], D. Goupilliere[o], S.R. Gozzini[c], R. Gracia[ah], K. Graf[ah], C. Guidi[ap,ad], B. Guillon[o], M. Gutiérrez[aq], H. van Haren[ar], A. Heijboer[r], A. Hekalo[am], L. Hennig[ah], J.J. Hernández-Rey[c], F. Huang[d], W. Idrissi Ibnsalih[e], G. Illuminati[s], C.W. James[al], M. de Jong[as,r], P. de Jong[ab,r], B.J. Jung[r], P. Kalaczyński[at,be], O. Kalekin[ah], U.F. Katz[ah], N.R. Khan Chowdhury[c], A. Khatun[q], G. Kistauri[av,au], C. Kopper[ah], A. Kouchner[aw,n], V. Kulikovskiy[ad], R. Kvatadze[av], M. Labalme[o], R. Lahmann[ah], G. Larosa[w], C. Lastoria[d], A. Lazo[c], S. Le Stum[d], G. Lehaut[o], E. Leonora[a], N. Lessing[c], G. Levi[t,s], M. Lindsey Clark[n], F. Longhitano[a], J. Majumdar[r], L. Malerba[ad], F. Mamedov[p], J. Mańczak[c], A. Manfreda[e], M. Marconi[ap,ad], A. Margiotta[t,s], A. Marinelli[e,f], C. Markou[i], L. Martin[k], J.A. Martínez-Mora[l], F. Marzaioli[u,e], M. Mastrodicasa[ae,g], S. Mastroianni[e], S. Miccichè[w], G. Miele[f,e], P. Migliozzi[e], E. Migneco[w], M.L. Mitsou[e], C.M. Mollo[e], L. Morales-Gallegos[u,e], C. Morley-Wong[al], A. Moussa[y], I. Mozun Mateo[ay,ax], R. Muller[r], M.R. Musone[e,u], M. Musumeci[w], L. Nauta[r], S. Navas[aq], A. Nayerhoda[ak], C.A. Nicolau[g], B. Nkosi[ai], B. Ó Fearraigh[ab,r], V. Oliviero[f,e], A. Orlando[w], E. Oukacha[n], D. Paesani[w], J. Palacios González[c], G. Papalashvili[au], V. Parisi[ap,ad], E.J. Pastor Gomez[c], A.M. Păun[aa], G.E. Păvălaş[aa], S. Peña Martínez[n], M. Perrin-Terrin[d], J. Perronnel[o], V. Pestel[ay], R. Pestes[n], P. Piattelli[w], C. Poirè[z,e], V. Popa[aa], T. Pradier[b], S. Pulvirenti[w], G. Quéméner[o], C. Quiroz[l], U. Rahaman[c], N. Randazzo[a], R. Randriatoamanana[k], S. Razzaque[az], I.C. Rea[e], D. Real[c], S. Reck[ah], G. Riccobene[w], J. Robinson[x], A. Romanov[ap,ad], A. Šaina[c], F. Salesa Greus[c], D.F.E. Samtleben[as,r], A. Sánchez Losa[c,ak], S. Sanfilippo[w], M. Sanguineti[ap,ad], C. Santonastaso[ba,e], D. Santonocito[w], P. Sapienza[w], J. Schnabel[ah], J. Schumann[ah], H.M. Schutte[x], J. Seneca[r], N. Sennan[y], B. Setter[ah], I. Sgura[ak], R. Shanidze[au], Y. Shitov[p], F. Šimkovic[q], A. Simonelli[e], A. Sinopoulou[a], M.V. Smirnov[ah], B. Spisso[e], M. Spurio[t,s], D. Stavropoulos[i], I. Štekl[p], M. Taiuti[ap,ad], Y. Tayalati[m], H. Tedjditi[ad], H. Thiersen[x], I. Tosta e Melo[a,aj], B. Trocmé[n], V. Tsourapis[i], E. Tzamariudaki[i], A. Vacheret[o], V. Valsecchi[w], V. Van Elewyck[aw,n], G. Vannoye[d], G. Vasileiadis[bb], F. Vazquez de Sola[r], C. Verilhac[n], A. Veutro[g,ae], S. Viola[w], D. Vivolo[u,e], J. Wilms[bc], E. de Wolf[ab,r], H. Yepes-Ramirez[l], G. Zarpapis[i], S. Zavatarelli[ad], A. Zegarelli[g,ae], D. Zito[w], J.D. Zornoza[c], J. Zúñiga[c], and N. Zywucka[x].

[a]INFN, Sezione di Catania, Via Santa Sofia 64, Catania, 95123 Italy
[b]Université de Strasbourg, CNRS, IPHC UMR 7178, F-67000 Strasbourg, France
[c]IFIC - Instituto de Física Corpuscular (CSIC - Universitat de València), c/Catedrático José Beltrán, 2, 46980 Paterna, Valencia, Spain
[d]Aix Marseille Univ, CNRS/IN2P3, CPPM, Marseille, France
[e]INFN, Sezione di Napoli, Complesso Universitario di Monte S. Angelo, Via Cintia ed. G, Napoli, 80126 Italy
[f]Università di Napoli "Federico II", Dip. Scienze Fisiche "E. Pancini", Complesso Universitario di Monte S. Angelo, Via Cintia ed. G, Napoli, 80126 Italy
[g]INFN, Sezione di Roma, Piazzale Aldo Moro 2, Roma, 00185 Italy
[h]Universitat Politècnica de Catalunya, Laboratori d'Aplicacions Bioacústiques, Centre Tecnològic de Vilanova i la Geltrú, Avda. Rambla Exposició, s/n, Vilanova i la Geltrú, 08800 Spain
[i]NCSR Demokritos, Institute of Nuclear and Particle Physics, Ag. Paraskevi Attikis, Athens, 15310 Greece
[j]University of Granada, Dept. of Computer Architecture and Technology/CITIC, 18071 Granada, Spain
[k]Subatech, IMT Atlantique, IN2P3-CNRS, Université de Nantes, 4 rue Alfred Kastler - La Chantrerie, Nantes, BP 20722 44307 France
[l]Universitat Politècnica de València, Instituto de Investigación para la Gestión Integrada de las Zonas Costeras, C/ Paranimf, 1, Gandia, 46730 Spain
[m]University Mohammed V in Rabat, Faculty of Sciences, 4 av. Ibn Battouta, B.P. 1014, R.P. 10000 Rabat, Morocco
[n]Université Paris Cité, CNRS, Astroparticule et Cosmologie, F-75013 Paris, France
[o]LPC CAEN, Normandie Univ, ENSICAEN, UNICAEN, CNRS/IN2P3, 6 boulevard Maréchal Juin, Caen, 14050 France
[p]Czech Technical University in Prague, Institute of Experimental and Applied Physics, Husova 240/5, Prague, 110 00 Czech Republic
[q]Comenius University in Bratislava, Department of Nuclear Physics and Biophysics, Mlynska dolina F1, Bratislava, 842 48 Slovak Republic
[r]Nikhef, National Institute for Subatomic Physics, PO Box 41882, Amsterdam, 1009 DB Netherlands
[s]INFN, Sezione di Bologna, v.le C. Berti-Pichat, 6/2, Bologna, 40127 Italy
[t]Università di Bologna, Dipartimento di Fisica e Astronomia, v.le C. Berti-Pichat, 6/2, Bologna, 40127 Italy
[u]Università degli Studi della Campania "Luigi Vanvitelli", Dipartimento di Matematica e Fisica, viale Lincoln 5, Caserta, 81100 Italy
[v]E. A. Milne Centre for Astrophysics, University of Hull, Hull, HU6 7RX, United Kingdom

[w] INFN, Laboratori Nazionali del Sud, Via S. Sofia 62, Catania, 95123 Italy
[x] North-West University, Centre for Space Research, Private Bag X6001, Potchefstroom, 2520 South Africa
[y] University Mohammed I, Faculty of Sciences, BV Mohammed VI, B.P. 717, R.P. 60000 Oujda, Morocco
[z] Università di Salerno e INFN Gruppo Collegato di Salerno, Dipartimento di Fisica, Via Giovanni Paolo II 132, Fisciano, 84084 Italy
[aa] ISS, Atomistilor 409, Măgurele, RO-077125 Romania
[ab] University of Amsterdam, Institute of Physics/IHEF, PO Box 94216, Amsterdam, 1090 GE Netherlands
[ac] TNO, Technical Sciences, PO Box 155, Delft, 2600 AD Netherlands
[ad] INFN, Sezione di Genova, Via Dodecaneso 33, Genova, 16146 Italy
[ae] Università La Sapienza, Dipartimento di Fisica, Piazzale Aldo Moro 2, Roma, 00185 Italy
[af] Università di Bologna, Dipartimento di Ingegneria dell'Energia Elettrica e dell'Informazione "Guglielmo Marconi", Via dell'Università 50, Cesena, 47521 Italia
[ag] Cadi Ayyad University, Physics Department, Faculty of Science Semlalia, Av. My Abdellah, P.O.B. 2390, Marrakech, 40000 Morocco
[ah] Friedrich-Alexander-Universität Erlangen-Nürnberg (FAU), Erlangen Centre for Astroparticle Physics, Nikolaus-Fiebiger-Straße 2, 91058 Erlangen, Germany
[ai] University of the Witwatersrand, School of Physics, Private Bag 3, Johannesburg, Wits 2050 South Africa
[aj] Università di Catania, Dipartimento di Fisica e Astronomia "Ettore Majorana", Via Santa Sofia 64, Catania, 95123 Italy
[ak] INFN, Sezione di Bari, via Orabona, 4, Bari, 70125 Italy
[al] International Centre for Radio Astronomy Research, Curtin University, Bentley, WA 6102, Australia
[am] University Würzburg, Emil-Fischer-Straße 31, Würzburg, 97074 Germany
[an] Western Sydney University, School of Computing, Engineering and Mathematics, Locked Bag 1797, Penrith, NSW 2751 Australia
[ao] IN2P3, LPC, Campus des Cézeaux 24, avenue des Landais BP 80026, Aubière Cedex, 63171 France
[ap] Università di Genova, Via Dodecaneso 33, Genova, 16146 Italy
[aq] University of Granada, Dpto. de Física Teórica y del Cosmos & C.A.F.P.E., 18071 Granada, Spain
[ar] NIOZ (Royal Netherlands Institute for Sea Research), PO Box 59, Den Burg, Texel, 1790 AB, the Netherlands
[as] Leiden University, Leiden Institute of Physics, PO Box 9504, Leiden, 2300 RA Netherlands
[at] National Centre for Nuclear Research, 02-093 Warsaw, Poland
[au] Tbilisi State University, Department of Physics, 3, Chavchavadze Ave., Tbilisi, 0179 Georgia
[av] The University of Georgia, Institute of Physics, Kostava str. 77, Tbilisi, 0171 Georgia
[aw] Institut Universitaire de France, 1 rue Descartes, Paris, 75005 France
[ax] IN2P3, 3, Rue Michel-Ange, Paris 16, 75794 France
[ay] LPC, Campus des Cézeaux 24, avenue des Landais BP 80026, Aubière Cedex, 63171 France
[az] University of Johannesburg, Department Physics, PO Box 524, Auckland Park, 2006 South Africa
[ba] Università degli Studi della Campania "Luigi Vanvitelli", CAPACITY, Laboratorio CIRCE - Dip. Di Matematica e Fisica - Viale Carlo III di Borbone 153, San Nicola La Strada, 81020 Italy
[bb] Laboratoire Univers et Particules de Montpellier, Place Eugène Bataillon - CC 72, Montpellier Cédex 05, 34095 France
[bc] Friedrich-Alexander-Universität Erlangen-Nürnberg (FAU), Remeis Sternwarte, Sternwartstraße 7, 96049 Bamberg, Germany
[bd] Université de Haute Alsace, rue des Frères Lumière, 68093 Mulhouse Cedex, France
[be] AstroCeNT, Nicolaus Copernicus Astronomical Center, Polish Academy of Sciences, Rektorska 4, Warsaw, 00-614 Poland

Acknowledgements

The authors acknowledge the financial support of the funding agencies: Agence Nationale de la Recherche (contract ANR-15-CE31-0020), Centre National de la Recherche Scientifique (CNRS), Commission Européenne (FEDER fund and Marie Curie Program), LabEx UnivEarthS (ANR-10-LABX-0023 and ANR-18-IDEX-0001), Paris Île-de-France Region, France; Shota Rustaveli National Science Foundation of Georgia (SRNSFG, FR-22-13708), Georgia; The General Secretariat of Research and Innovation (GSRI), Greece Istituto Nazionale di Fisica Nucleare (INFN), Ministero dell'Università e della Ricerca (MIUR), PRIN 2017 program (Grant NAT-NET 2017W4HA7S) Italy; Ministry of Higher Education, Scientific Research and Innovation, Morocco, and the Arab Fund for Economic and Social Development, Kuwait; Nederlandse organisatie voor Wetenschappelijk Onderzoek (NWO), the Netherlands; The National Science Centre, Poland (2021/41/N/ST2/01177); The grant "AstroCeNT: Particle Astrophysics Science and Technology Centre", carried out within the International Research Agendas programme of the Foundation for Polish Science financed by the European Union under the European Regional Development Fund; National Authority for Scientific Research (ANCS), Romania; Grants PID2021-124591NB-C41, -C42, -C43 funded by MCIN/AEI/ 10.13039/501100011033 and, as appropriate, by "ERDF A way of making Europe", by the "European Union" or by the "European Union NextGenerationEU/PRTR", Programa de Planes Complementarios I+D+I (refs. ASFAE/2022/023, ASFAE/2022/014), Programa Prometeo (PROMETEO/2020/019) and GenT (refs. CIDEGENT/2018/034, /2019/043, /2020/049. /2021/23) of the Generalitat Valenciana, Junta de Andalucía (ref. SOMM17/6104/UGR, P18-FR-5057), EU: MSC program (ref. 101025085), Programa María Zambrano (Spanish Ministry of Universities, funded by the European Union, NextGenerationEU), Spain; The European Union's Horizon 2020 Research and Innovation Programme (ChETEC-INFRA - Project no. 101008324).